SPECIFIC ANGULAR MOMENTUM CORRELATION
WITH THE NUMBER OF SATELLITES

ANA LALOVIĆ ⦿, MILENA JOVANOVIĆ ⦿, SLADJANA KNEŽEVIĆ ⦿
and SRDJAN SAMUROVIĆ ⦿

Astronomical Observatory, Volgina 7, 11060 Belgrade, Serbia
E–mail: ana@aob.rs

Abstract. The number of satellites is correlated with the mass of the galaxy bulge and bulge-to-total ratio, indicating that the origin of satellites might be related to the mechanism responsible for bulge creation/growth. In this work, we have found that specific angular momentum correlates positively with the number of satellites for a sample of six nearby galaxies for which we have a complete census of the satellite population. Contrary to our previous work where we found a negative correlation using an approximate formula for specific angular momentum, in this work we have measured specific angular momentum more thoroughly: using both rotation curve data and galaxy mass distribution in the near infrared. Disagreement can be explained by the difference between approximate and more accurate measurements of angular momentum.

1. INTRODUCTION

According to the Λ cold dark matter model (ΛCDM), galaxies formed inside dark matter halos where baryons were mixed with dark matter particles and shared the same angular momentum. After cooling and decoupling from dark matter, baryons collapsed into stellar structures retaining angular momentum. The conservation of angular momentum allows us to trace galaxy evolution back to the earliest stages of formation. The other two fundamental properties are mass and energy. Unlike mass and angular momentum, energy could be lost through dissipative collapse and radiation. The relation between mass and specific angular momentum (normalized to mass) is the so-called Fall relation (Fall 1983). It relates two fundamental galaxy properties that are being conserved and are independent. Romanowsky & Fall (2012) revisited the Fall relation, incorporating a larger sample of galaxies with diverse morphology. While spiral galaxies lie along the well-defined sequence with very little scatter, early-type galaxies form another sequence, parallel to the former one, but with a lower intercept. Galaxy morphology is reflected in the bulge-to-total (B/T) ratio since each galaxy can be considered as the combination of a bulge and a disk, thus the Fall relation can be considered as the Hubble sequence represented by fundamental, conserved, and independent galaxy properties.

One of the major challenges to the concordance cosmology is the number of satellites and in particular their distribution around host galaxies (Klypin et al. 1999, Pawlowski & Kroupa 2013, Müller et al. 2018). We can pose another question - is the number of satellites related to the other fundamental properties, in particular galaxy mass and angular momentum? And what are the implications of such correlations?

Kroupa et al. (2010) found a correlation between the number of satellites and the mass of the galaxy bulge, while Javanmardi & Kroupa (2020) found another correlation between the B/T ratio and the number of satellites. These findings can be interpreted in the following way: the process responsible for bulge formation and its growth imprinted in the galaxy morphology (through B/T) is also related to the formation of satellites. The same process may be responsible for building up the galaxy bulge while creating the satellites. If we assume that all galaxies in a certain mass range harbor a similar number of satellites, then bulge growth through minor merges should have left a sparse satellite population, which is quite opposite to the recent findings - the more massive the bulge is, the more satellites have been detected. In this work, we have tested if the specific angular momentum is also related to the number of satellites (N_{sat}), and we discuss the implications. In our previous work (Vudragović et al. 2022), we found an opposite (negative) correlation between these two properties, but the specific angular momentum was estimated using approximate formula and the number of satellites was limited only to the brightest satellites. Here, for the first time, we have obtained precise (not approximate) measurements of the specific angular momentum and the actual total number of satellites.

2. SAMPLE

We have used the same sample of galaxies as Javanmardi & Kroupa (2020) (excluding the Milky Way) because it already includes a complete census of the satellite population, which is difficult to obtain. Only for several nearby galaxies through decades of demanding spectroscopic observations satellites are being confirmed. The selected galaxies are: M31, M33, M81, M94, M101 and Centaurus A (CenA, hereafter). We have excluded the Milky Way galaxy since we need homogeneous data for mass distribution of all sample galaxies, that is derived from near infrared photometry obtained with Spitzer Space Telescope, that we cannot have for our galaxy given that we are inside it.

Specific angular momentum is angular momentum normalized by the galaxy mass. In Romanowsky & Fall (2012) specific angular momentum has been expressed by the quantities that can be acquired from observations: rotation velocity (v_{rot}) and surface density profile (Σ) along the galaxy semimajor axis (x):

$$\vec{j} = C_i \frac{\int v_{rot}\ \Sigma(x)\ x^2\ dx}{\int \Sigma(x)\ x\ dx},\ C_i \simeq \frac{0.99 + 0.14\ i}{\sin(i)}. \tag{1}$$

The coefficient C_i depends on the geometry but can be approximated as the function of inclination i.

Rotation velocity is most frequently derived from HI observations. In addition, it can be derived from CO molecular lines and/or Hα spectroscopy for inner parts of the galaxy. We have downloaded rotation velocity distribution from the archive[1] maintained by Yoshiaki Sofue (Sofue et al. 1999) based on both optical and radio data. For all spiral sample galaxies, we have retrieved rotation velocity distribution along the galaxy's semimajor axis. One of the galaxies is early-type and its kinematics is taken from Wilkinson et al. (1986) and Peng et al. (2004) including spectroscopy and planetary nebulae data.

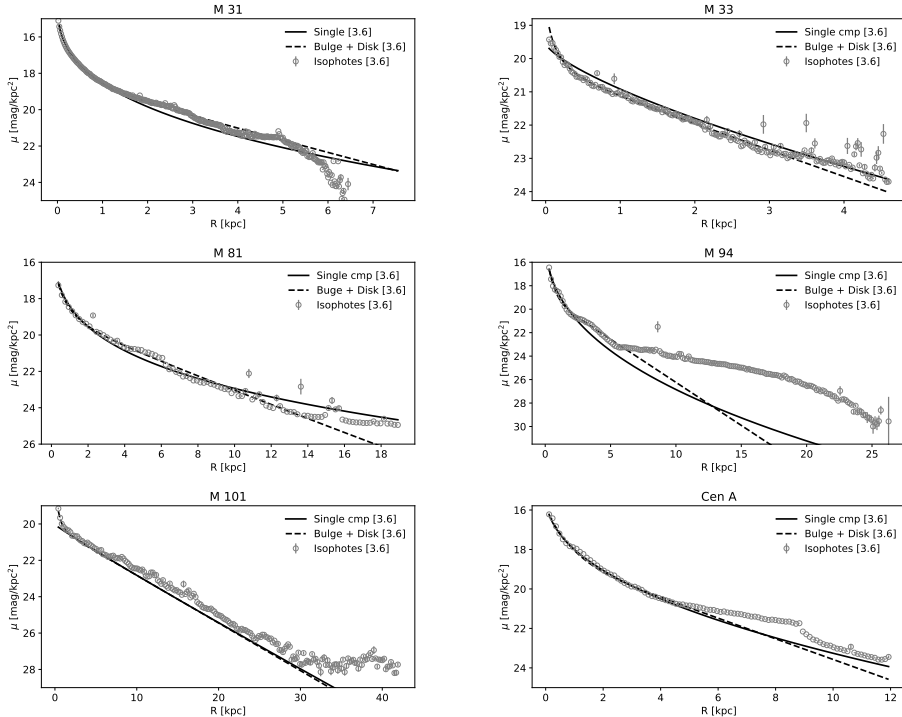[1]`http://www.ioa.s.u-tokyo.ac.jp/~sofue/`

Figure 1: Surface brightness profiles of sample galaxies in the near-infrared. All galaxies are modeled with a single Sérsic component (tick line), but also with two components - a bulge and a disk (dashed line). Grey points are obtained from 3.6 μm-band, measuring average intensity inside concentric ellipses with the `IRAF's ellipse` procedure.

Surface brightness profile should correspond to the mass distribution and since the near-infrared light best traces old stellar population that makes most of the galaxy's stellar mass, we used Spitzer's observations in 3.6 μm. We have downloaded images of our sample galaxies from the Spitzer Heritage Archive[2].

3. RESULTS

Near-infrared images are modelled with `Galfit` code (Peng et al. 2010) with single and two components (a bulge and a disk). Single-component fits are as good as two-component fits as can be seen in Figure 1, and will be used to measure mass distribution. As a side note, galaxy M 94 has prominent spiral arms that cannot be modelled by Sérsic law and thus the fit projected along the major axis is not successful (Figure 1), but since the bulk of the mass is in the bulge and disk this is not relevant for our study. Structural parameters of single-component fit including Sérsic index and effective radius are used to calculate $\Sigma(x)$, which is given by the simple Sérsic

---

[2]`https://sha.ipac.caltech.edu/applications/Spitzer/SHA/`

Table 1: Structural parameters obtained from modelling near-infrared images with Sérsic law: (1) Galaxy name; (2) Number of satellites (N_{sat}) within 200 kpc from the host galaxy, taken from Javanmardi & Kroupa (2020); (3) Distance to the galaxy in Mpc; (4) effective radius from the single component Sérsic fit; (5) sine value of galaxy inclination; (6) Sérsic index n; (7) logarithm of the cumulative distribution of the specific angular momentum corrected for galaxy inclination (plateau value).

Name	N_{sat}	Distance [Mpc]	R_{eff} [kpc]	$\sin(i)$	n	$\log j$ [km s^{-1} kpc]
M31	17	0.69	1.9	0.73	2.91	3.68
M33	0	0.79	2.56	0.94	1.4	2.62
M81	16	3.25	4.41	0.79	4.46	3.41
M94	2	5.1	0.87	0.51	2.46	3.08
M101	8	7.2	6.81	0.46	1.05	3.47
CenA	27	4.1	2.64	0.37	2.16	3.69

law required to measure specific angular momentum using Equation 1, and are given in the Table 1.

Cumulative distribution of angular momentum, i.e. $v_{rot} \Sigma(x) x^2$ was calculated by integrating Sérsic law for a particular galaxy up to the distance from the galaxy center for which the rotation velocity is provided point-by-point (discrete distribution in rotation velocity). The total angular momentum is taken as the last point in the cumulative distribution of angular momentum along the galaxy semimajor axis and is given in Table 1. The distribution of the specific angular momentum is visualized in Figure 2, along with the distribution of rotation velocity. The total momentum is encapsulated if and only if the plateau is reached which is not the case for all galaxies. Depending on the value of the Sérsic index, kinematics needs to extend to more effective radii in order to reach the desired plateau value of angular momentum. The vertical dashed line in Figure 2 represents the measured effective radius for each galaxy. The kinematics of three galaxies (M33, M101, and M81) is insufficiently deep to reach the desired, plateau value. However, since the galaxy sample is very modest, we have decided to keep all the measured quantities. Finally, we can relate the number of satellites to the total specific angular momentum using measurements from Table 1. In Figure 3 all sample galaxies show a positive correlation meaning that galaxies that harbor more satellites have higher specific angular momentum.

4. SUMMARY

We have measured the total specific angular momentum for the sample of 6 nearby galaxies for which we have the overall number of satellites from the literature (Javanmardi & Kroupa 2020). The correlation between the two properties is positive, i.e. galaxies with larger specific angular momentum have more satellites regardless of their overall mass, since the angular momentum is normalized to the total mass of host galaxies. Angular momentum is conserved physical property inherited from dark matter halo in which galaxy is initially formed along with satellites. If, due to dynamical friction satellites slow down in time and merge with host galaxy growing a galaxy bulge, then their number should be negatively correlated with the mass of the bulge, and also with the angular momentum. Since the number of satellites is also
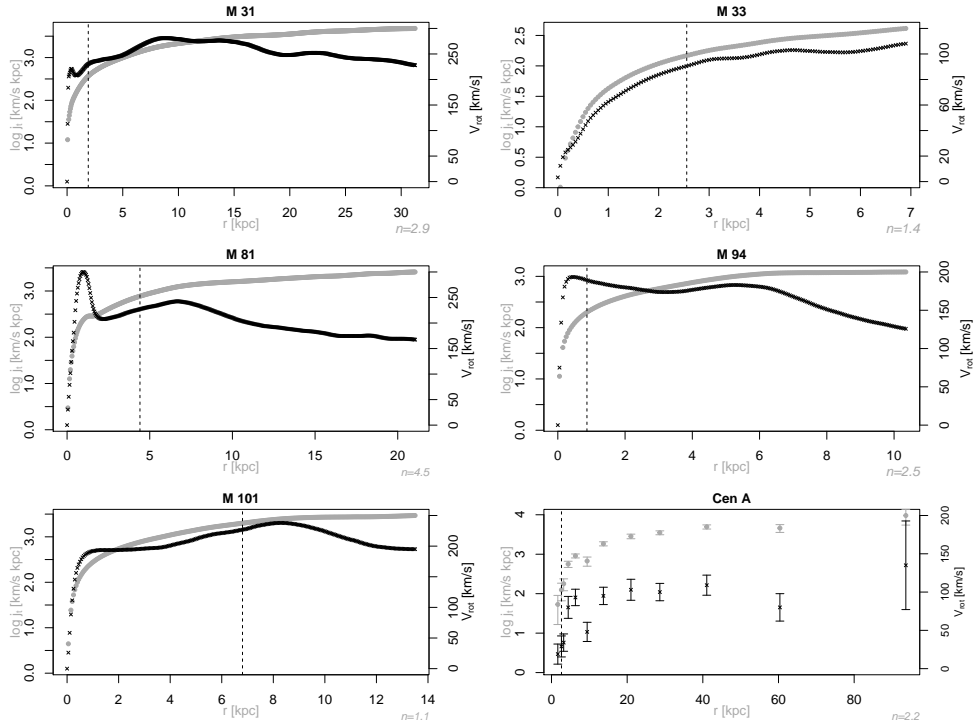
Figure 2: Cumulative distribution of specific angular momentum (grey) and rotation velocity (black) for all sample galaxies is given. A dashed vertical line is the effective radius given in Table 1. At the bottom right corner the Sérsic index n is indicated for each galaxy.
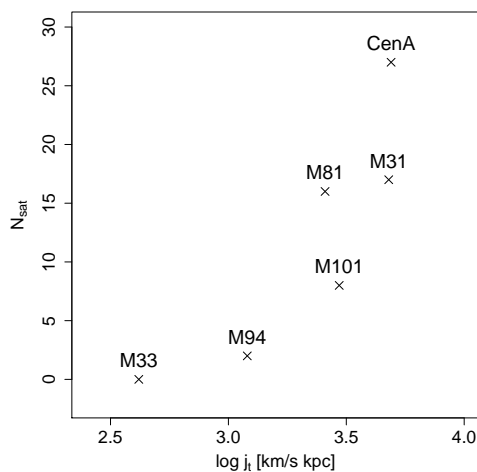

Figure 3: The number of satellites vs. total specific angular momentum for our sample galaxies

.

positively correlated with the mass of the bulge (Kroupa et al. 2010) and bearing in mind that satellites are mainly distributed along thin planes (Pawlowski & Kroupa 2013) this could be an indication that a major merger contributed both to the bulge growth and to the formation of satellites along the plane of collision. The consequence of this would be that satellites are formed at the time of the merger event and this will be the subject of some future work.

Acknowledgements

References

Fall, S. M.: 1983, in Internal Kinematics and Dynamics of Galaxies, ed. E. Athanassoula, Vol. 100, 391–398.

Javanmardi, B. & Kroupa, P.: 2020, *MNRAS*, **493**, L44.

Klypin, A., Kravtsov, A. V., Valenzuela, O., & Prada, F.: 1999, *ApJ*, **522**, 82. [LINK]

Kroupa, P., Famaey, B., de Boer, K. S., Dabringhausen, J., Pawlowski, M. S., Boily, C. M., Jerjen, H., Forbes, D., Hensler, G., & Metz, M.: 2010, *A&A*, **523**, A32.

Müller, O., Pawlowski, M. S., Jerjen, H., & Lelli, F.: 2018, *Science*, **359**, 534.

Pawlowski, M. S. & Kroupa, P.: 2013, *MNRAS*, **435**, 2116. [LINK]

Peng, C. Y., Ho, L. C., Impey, C. D., & Rix, H.-W.: 2010, *AJ*, **139**, 2097.

Peng, E. W., Ford, H. C., & Freeman, K. C.: 2004, *ApJ*, **602**, 685.

Romanowsky, A. J. & Fall, S. M.: 2012, *ApJS*, **203**, 17.

Sofue, Y., Tutui, Y., Honma, M., Tomita, A., Takamiya, T., Koda, J., & Takeda, Y.: 1999, *ApJ*, **523**, 136.

Vudragović, A., Petraš, I., Jovanović, M., Knežević, S., & Samurović, S.: 2022, *A&A*, **662**, A17.

Wilkinson, A., Sharples, R. M., Fosbury, R. A. E., & Wallace, P. T.: 1986, *MNRAS*, **218**, 297.